A Surface Plasmon Resonance Study of Volume Phase Transitions in *N*-Isopropylacrylamide Gel Films

Marianne E. Harmon,[†] Thomas A. M. Jakob,[‡] Wolfgang Knoll,[†,‡] and Curtis W. Frank*[,†]

Department of Chemical Engineering, Stanford University, Stanford, California 94305, and Max Planck Institute for Polymer Research, Ackermannweg 10, D-55128 Mainz, Germany

Received June 7, 2001; Revised Manuscript Received April 29, 2002

ABSTRACT: Cross-linked *N*-isopropylacrylamide (NIPAAm) gel is covalently attached to a substrate, and the resulting interface is probed using surface plasmon resonance (SPR) as a function of hydrostatic pressure and temperature. SPR provides a direct measurement of the local refractive index, which changes with the swelling ratio of the gel film. Similar to bulk NIPAAm gel, the transition temperature increases and the volume phase transition becomes broader as pressure increases. The width of the transition ranges from less than 0.5 °C at 1 bar to as much as 10 °C at 1000 bar, and the transition temperature increases by as much as 7 °C over the same range of pressures. However, the presence of a fixed substrate effectively confines the volume phase transition near the interface to one dimension, perpendicular to the substrate. This has significant effects on the transition temperature, particularly at high cross-linking density and high concentration of an ionizable comonomer. Furthermore, the swelling effect of the ionic groups is reduced, and the water content of the swollen gel does not change with increased ionic content. While the volume phase transition of the corresponding bulk gels can have a total volume change as large as 100-fold, the gel films have a total volume change around 15-fold.

Introduction

Hydrogels have been shown to respond to a variety of stimuli such as pH,[1] temperature,[2] magnetic fields,[3] and electric fields[4] and have been proposed for use in a wide range of applications, particularly within the biological sciences. These include drug delivery systems,[5] artificial muscles,[6] membrane separations,[7] and surfaces in biomaterials.[8] Thermoresponsive polymer gels are known to have a volume phase transition, analogous to the lower critical solution temperature (LCST) of the corresponding linear polymer. The volume phase transition can be modeled using Flory−Tanaka theory as a balance between mixing free energy, rubber elasticity free energy, and osmotic pressure due to counterions of ionizable comonomers.[9] However, this understanding of bulk gels does not necessarily extend to the many applications of thermoresponsive polymer gels. When the gel is used in actual devices, the volume phase transition is inevitably constrained in some way and no longer corresponds to theoretical predictions.

N-Isopropylacrylamide (NIPAAm) gel has been studied extensively, and through the addition of ionizable comonomers such as sodium acrylate (SA), the total volume change can be increased to as much as 100-fold along with an elevated transition temperature.[9] In work by Suzuki and co-workers,[10,11] the volume phase transition has been limited to two dimensions by fixing the ends of cylindrical NIPAAm gels. As a result of this constraint, neutral NIPAAm gel has a larger total volume change and higher volume phase transition temperature. This behavior can also be modeled theoretically through a two-dimensional analogue of existing theory and modifications that allow for the resulting non-Gaussian chain conformations.[10,11]

The LCST transition results from a delicate balance of hydrophobic and hydrophilic groups within the polymer.[12] Hydrogen bonding is central to understanding the volume phase transition in hydrogels, and added salts or urea can significantly alter the transition by acting as structure breakers. Applying hydrostatic pressure to bulk gel has similar effects in that the hydrogen-bonding environment is disrupted. As a result, the transition temperature increases, and the discontinuous transition becomes continuous with a broader transition as the pressure is increased.[13−15] The LCST reported for linear NIPAAm polymers is 32 °C and is usually defined as the onset of the transition in differential scanning calorimetry (DSC)[16,17] or cloud point measurements.[12,18] The swelling ratio and volume phase transition temperature of cross-linked NIPAAm gel are known to be influenced by the gel microstructure and are strong functions of the synthesis conditions.[19] Furthermore, the volume phase transition changes from continuous to discontinuous as the gel network characteristics change.[20] The reported value of the transition temperature also varies according to the measurement technique used and tends to be lower for DSC measurements, where it is defined as the onset of the transition, than for swelling ratio measurements, where it is defined as the midpoint of the transition.[17]

Surface plasmon resonance spectroscopy (SPR) is surface-sensitive due to the evanescent field of the surface plasmon.[21] The latter is an electromagnetic wave traveling along the interface between a metal and a dielectric. Its electric field decays exponentially into both materials over a distance of a few hundred nanometers, and the wave has a finite propagation length due to damping processes in the metal. The resulting data are a direct measure of the local average refractive index of the dielectric close to the surface, and with Fresnel calculations either the thickness or the refractive index of thin films at an interface can be determined. Fur-

[†] Stanford University.
[‡] Max Planck Institute for Polymer Research.
* To whom correspondence should be addressed. E-mail: curt@chemeng.stanford.edu.

10.1021/ma010985k CCC: $22.00
Published on Web 06/21/2002

thermore, a time-dependent measurement mode enables the detection of changes in the local average dielectric constant due to the adsorption of molecules onto the surface or changes in film properties due to an external trigger. SPR studies of linear polymers in thin films and at interfaces have shown that the resulting confinement can alter characteristic transitions that exist in the bulk materials. Examples include the glass transition temperature,[22] the LCST of linear substituted acrylamides,[23] and nematic transitions in polymers with liquid crystalline side chains.[24]

Although the LCST transition of linear polymers has been observed at an interface,[23] the more common cross-linked hydrogels have only been examined on a more macroscopic scale. Bulk gel is usually weighed to determine the solvent content and swelling ratio under various conditions.[2] Alternatively, the gel is observed using a camera or microscope to determine the degree of swelling in response to different stimuli.[10,11,25] This approach is clearly limited to larger gel samples and is not applicable to the observation of thin gel films. Because of its surface sensitivity and suitability for the study of thin films, we have used SPR to determine the refractive index of gel films as a function of temperature and hydrostatic pressure. The swelling ratio can then be determined through the known relationship of polymer volume fraction and refractive index of the gel.

Thin films of linear poly-NIPAAm have been used to create responsive surfaces for a wide range of applications.[26] The preparation of these films includes techniques such as surface grafting,[27−29] plasma polymerization,[26] and photopolymerization.[30] The resulting transition temperatures and swelling behavior vary greatly, even when the graft architecture and morphology of the film are well-known.[27] Linear poly-NIPAAm has also been grafted to latex particles,[31] and cross-linked NIPAAm gel has been used to form thermoresponsive core−shell colloids.[32,33] The results from scattering experiments with these core−shell colloids are particularly interesting because the presence of a fixed interface between the shell and the core was found to limit the degree of swelling of the thermoresponsive shell.

If a cross-linked gel is chemisorbed to the substrate, it will be unable to expand and contract laterally, effectively confining the transition to one dimension, perpendicular to the substrate.[25,34] This paper examines how this type of confinement affects the transition temperature and the total volume change of both neutral and ionized NIPAAm gels.

Experimental Section

Materials. All materials employed were of research grade and were used as received from commercial sources without any additional purification unless indicated otherwise. *N*-Isopropylacrylamide (NIPAAm), sodium acrylate (SA), *N*,*N*′-methylenebis(acrylamide) (BIS cross-linker), ammonium persulfate (APS initiator), *N*,*N*,*N*′,*N*′-tetramethylethylenediamine (TEMED accelerator), and γ-methacryloxypropyltrimethoxysilane were purchased from Sigma-Aldrich, Germany. 4,4′-Azobis(4-cyanopentanoic acid), thionyl chloride, triethylamine, dichloromethane, 3-(aminopropyl)triethoxysilane, and toluene were purchased from Sigma-Aldrich and were dried prior to use according to standard procedures.[35]

Sample Preparation. Photolithographically structured quartz samples were prepared by reactive ion etching to produce a grating structure of roughly 506 nm grating spacing on the top surface; subsequently, approximately 150 nm of gold was deposited by thermal evaporation. A sol−gel process was used to deposit a 15 nm layer of silica on the gold surface. This synthesis has been described previously along with the effects of both the gold and silica layers under hydrostatic pressure.[36]

Spacer Technique. The silica layer was treated with γ-methacryloxypropyltrimethoxysilane, and thin films of NIPAAm gel were cast using Teflon spacers according to the procedure of Zheng and co-workers.[37] The pregel solution was prepared by dissolving NIPAAm (700−630 mM), SA (0−70 mM), BIS (3.5−15 mM), and TEMED (20 μL) in 3 mL of Milli-Q water and then degassing by at least three consecutive freeze−thaw cycles. A 60 μL aliquot of a 40 mg/mL solution of APS in Milli-Q water was added to initiate the polymerization. The total gel concentration was kept constant, with the sum of the SA and NIPAAm concentrations equaling 700 mM. The thickness of the resulting gel films was 40 μm in the swollen state and 4 μm in the collapsed state, as determined by profilometry. This thickness is much larger than the decay length of the surface plasmons into the dielectric, so the plasmon mode is only sensitive to the gel−substrate interface, and the gel can be modeled as an infinite medium.

UV Technique. A surface-bound initiator was used to vary the NIPAAm gel film thickness. NIPAAm cannot be polymerized above the LCST without significantly altering the properties of the resulting gel, and this is conveniently avoided through the use of a photoinitiator. A symmetric surface-bound photoinitiator was synthesized through the reaction of 4,4′-azobis(4-cyanopentanoic acid) with thionyl chloride and a subsequent reaction of the 4,4′-azobis(4-cyanopentanoic acid chloride) with 3-(aminopropyl)triethoxysilane and triethylamine in dry dichloromethane. The triethylamine salt was removed by filtration to yield the azo initiator with a triethoxysilane group at both ends. This initiator can be chemisorbed to the silica layer through the silane groups and can be used to produce thin polymer films or patterns, through the use of appropriate masks.[38]

The surface functionalization was achieved through placing the sample in a Schlenck tube with a 1 mM solution of the photoinitiator in dry toluene. The sample was rinsed with toluene, dried with nitrogen gas, and transferred to another Schlenck tube with the pre-gel solution. The pre-gel solution was the same as the spacer technique but contained no APS or TEMED to initiate the polymerization. The Schlenck tube was purged with nitrogen and illuminated with a high-pressure Hg lamp to produce films of different thicknesses. The time for a 0.3 μm film varied with SA concentration and ranged from 5 min for 70 mM SA to 30 min for 0 mM SA. The resulting film thickness is on the order of the decay length of the surface plasmons into the dielectric, and the resulting measurements are of the entire film.

SPR Measurements. The grating coupling scheme was used for exciting surface plasmons in the case of the high-pressure measurements.[21,36,39] A more detailed description and schematic of the experimental setup can be found in ref 36. Here, we give only a short overview of the experimental technique. Surface plasmons are excited using p-polarized light, in this case, a He−Ne laser beam with a wavelength of 632.8 nm. The chopped beam is reflected off the gold-coated sample, which is mounted on a $\theta/2\theta$ goniometer, and the reflected intensity is then monitored by means of a photodiode that is read out by a lock-in amplifier. By varying the angle of incidence, typical reflectivity vs angle scans (see Figure 1A) can be recorded. The observed minimum corresponds to the excitation of a surface plasmon; i.e., the momentum and energy of the laser beam and the surface plasmon excitation are matched. For the high-pressure experiments, the pressure cell was connected to a syringe pump and controller to establish pressures up to 1000 bar with an accuracy of 2.5 bar in the optical cell. The temperature was varied using an electrical heating mantle that surrounded the cell. Cooling was achieved by means of water-cooled loops connected to a thermostat. A temperature controller maintained a constant temperature profile with an accuracy of 0.1 °C.

Transition Temperatures. The resulting angular scans were interpreted via Fresnel calculations to determine the

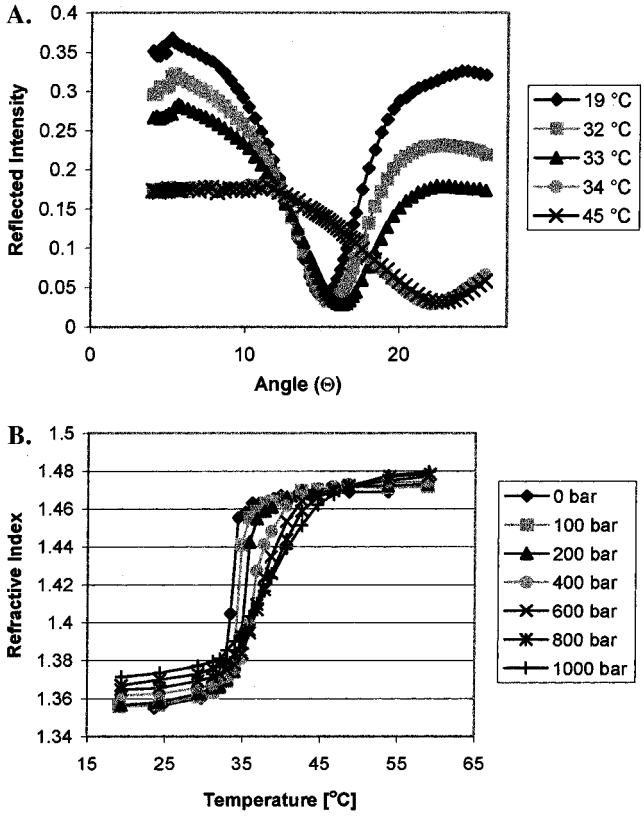

Figure 1. (A) SPR reflectivity scans showing the characteristic shape of the grating coupling scheme for a sample with 0 mM SA, 700 mM NIPAAm, and 3.5 mM BIS at 0 bar. The transition temperature is at 33.5 °C, and the angle of the resonance minimum shifts as a function of temperature. As the gel collapses, it also scatters more light, and the overall intensity drops. (B) The gel refractive index is graphed as a function of temperature and pressure for the same sample. Pressure was increased in 100 bar increments, but for clarity, not all curves are shown. Intermediate measurements follow the trends above.

refractive index of the gel film as a function of temperature and pressure. These data were fit to a sigmoidal curve, and the inflection point of the curve was defined as the transition temperature. Bulk gels were synthesized using the procedure of Tanaka and co-workers.[2,9] The resulting gels were cylindrical in shape, and the diameter of the cylinder was tracked as a function of temperature. For neutral bulk gels this curve is continuous, with the inflection point of the curve defined as the transition temperature, while for ionized bulk gels the curve has a discontinuity at the transition temperature.

All transitions were fully reversible, and we observed no hysteresis. Therefore, all measurements were recorded by increasing temperature and then varying pressure at constant temperature on a single sample. This method gave the same results as one in which the pressure was varied first, followed by the temperature, but accelerated the measurements dramatically. The equilibration time for the gel after each temperature and pressure change was determined in the SPR kinetic mode[21] and ranged from 10 to 25 min.

Results and Discussion

The phase behavior of the gel at the NIPAAm−substrate interface was observed as a function of temperature (approximately 15−65 °C) and pressure (1−1000 bar). In refs 36 and 39 it was shown that both the gold and the sol−gel withstand the applied pressure, and this constitutes the basis for the results presented here. The resulting scans (see Figure 1A) were fit to Fresnel calculations to determine the refractive index n of the gel. Note that the drop in reflected intensity outside the surface plasmon resonance and the angular broadening of the excitation are both due to increased scattering in the collapsed state of the gel.

Refractive Index. The refractive index can be correlated to the water content of the gel through a Lorentz−Lorenz calculation and the known relationship between refractive index and pressure.[39,40] The resulting data were quantified through fitting with a sigmoidal curve, using the parameters n(low temperature), n(high temperature), transition temperature T, and transition width ΔT. Figure 1B shows the refractive index as a function of temperature and pressure for one such sample. Following the curve at 0 bar, the refractive index changes from $n(T = 18\ °C)$ of 1.355, which corresponds to a gel swollen with water, to $n(T = 60\ °C)$ of 1.469, which corresponds to a collapsed and hydrophobic gel phase containing little water. At both low and high temperatures, the refractive index also changes as a function of pressure due to the increased density of both water and polymer at increased pressure.

To illustrate this effect, the refractive index data at 19.3 and 53.8 °C were fitted using a combination of the Lorentz−Lorenz and the Tait equations to give the Tait parameter $B(T)$ and the Lorentz−Lorenz constant R_{LL} (see Figure 2). From the Tait parameter the isothermal compressibility $\kappa_0(T)$ can then easily be calculated.[39,41] However, the resulting values, $\kappa_0(19.3\ °C) = 560 \times 10^{-6}$ MPa^{-1} and $\kappa_0(53.8\ °C) = 140 \times 10^{-6}$ MPa^{-1}, should only be treated as approximate values. Both equations rely on approximations that have proved to hold well for certain liquids and polymers but also have their drawbacks, e.g., in the case of water.[42] A direct measurement of either density or volume change upon variation of temperature and pressure would therefore be preferred, but the above values are in good agreement with the literature for the swollen (water) state and the collapsed (polymer) state.

Volume Phase Transition. Similar to bulk NIPAAm gel, both the transition temperature T and the width of the transition ΔT increase as a function of pressure. This has been attributed to the disruption of the hydrogen-bonding environment within the gel, especially that surrounding the hydrophobic isopropyl group. The entropy of solution is decreased and causes the Flory interaction parameter χ to increase as a function of pressure. Both the transition temperature and the width of the transition increase as a result.[13,14] The broadening of the transition with increased pressure shown in Figure 1B is representative of the samples examined in this study. In general, the width of the transition ranged from less than 0.5 °C at 1 bar to as much as 10 °C at 1000 bar, and the transition temperature increased over the same range of pressures as shown in Figure 3. An unusual effect of this phase behavior is that under certain conditions increasing pressure can actually cause the gel to expand. In Figure 1B, for example, at 1 bar and 35 °C the gel is collapsed while at 1000 bar and 35 °C it is swollen. This unique phase behavior was found for all NIPAAm gel samples investigated as part of these experiments and has been found in bulk NIPAAm gel as well.[15]

Gel Composition. Table 1 shows the volume phase transition temperature at 1 bar as a function of ionizable comonomer (SA) concentration and cross-linking (BIS) density. As known from Flory−Tanaka theory, the

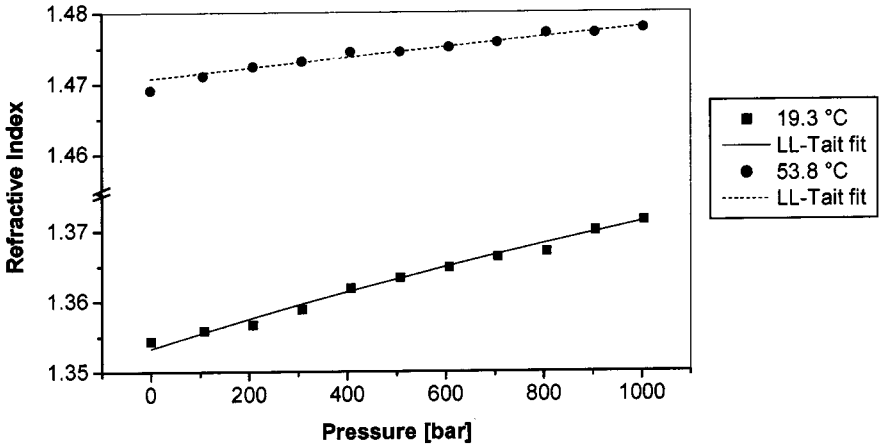

Figure 2. Refractive index of the gel is graphed as a function of pressure at 19.3 °C (squares) and 53.8 °C (circles) for a sample with 0 mM SA, 700 mM NIPAAm, and 3.5 mM BIS. The data were evaluated using the Lorentz−Lorenz equations (LL) combined with Tait's equations to give the compressibility of the gel in the swollen (19.3 °C, solid line) and the collapsed (53.8 °C, dotted line) state.

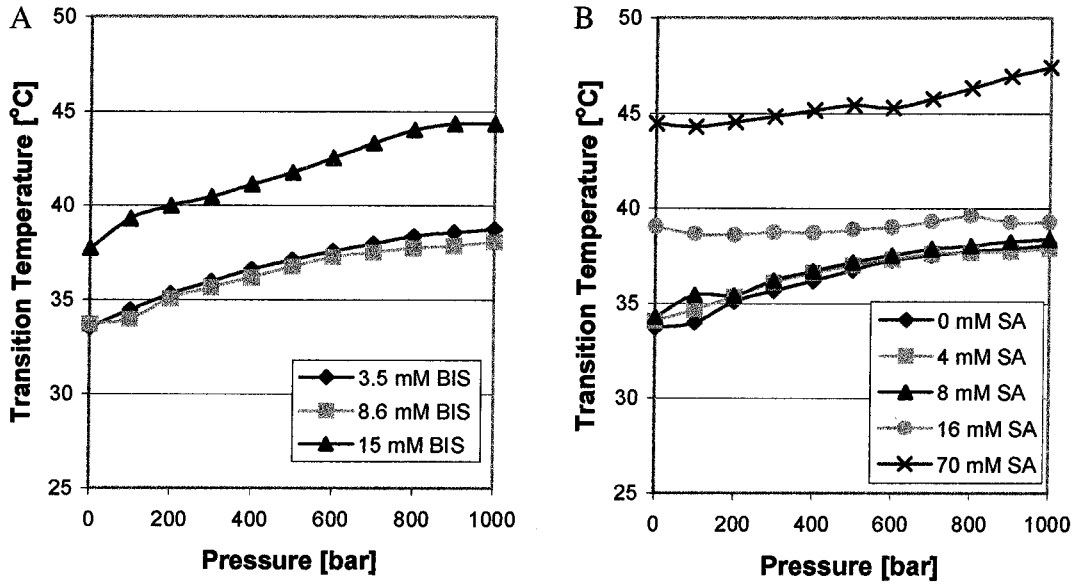

Figure 3. Pressure effects on the volume phase transition temperature of 4 μm films. (A) All samples have a gel composition of 0 mM SA and 700 mM NIPAAm with cross-linking density shown (mM BIS). (B) All samples have a cross-linking density of 8.6 mM BIS with ionizable comonomer concentration as shown (x mM SA). The corresponding NIPAAm concentration is (700 − x) mM, keeping the total gel network concentration constant.

Table 1. Volume Phase Transition Temperatures at 1 bar

		transition temperature [°C]		
SA [mM]	BIS [mM]	bulk gel	0.3 μm film[a]	4 μm film[b]
0	8.6	34.3	33.8	33.7
4	8.6	34.7		34.1
8	8.6	35.9		34.3
16	8.6	36.8	38.9	39.1
32	8.6	37.7	42.1	
70	8.6	41.9	44.8	44.5
0	3.5	34.2		33.5
0	15	34.4		37.7

[a] The 0.3 μm film (UV technique) measurements probe the entire film. [b] The 4 μm film (spacer technique) measurements are of the gel−substrate interface.

transition temperature of bulk NIPAAm gel increases as a function of the SA concentration but is largely unaffected by the cross-linking density. However, as illustrated by the data in Table 1, the gel at the NIPAAm−substrate interface shows further increase in the volume phase transition at higher SA and BIS concentrations. Furthermore, at lower SA and BIS concentrations, the transition temperature is slightly lower than the corresponding bulk samples. This is analogous to other studies that show the effect of confinement at a fixed substrate altering characteristic transitions in polymeric materials.[22−24] The swelling ratio and transition temperature of bulk gel are known to be influenced by the synthesis conditions. The procedure used for the preparation of the bulk gels and the method for determining the transition temperature are based on previously published results for the same system and are in good agreement with these data.[9] The agreement between the data using the spacer and UV techniques is surprisingly good, considering the differences in the synthesis conditions. However, the surface grafting density of the two systems should be similar, along with the gel network concentration and cross-linking density. Perhaps this is sufficient to give the gel films from the two techniques similar swelling ratios and transition temperatures in this confined geometry.

Comparing the effects of SA and BIS on the transition temperature, we note that SA concentration affects the

transition temperature in both the bulk gel and gel films while BIS concentration affects only the gel films. The gel films in this study are relatively loosely cross-linked, and although the gel−substrate interface is fixed, the gels are swollen with water and the individual polymer chains should have substantial mobility. However, as the cross-linking density increases, the modulus of the film increases, the mobility of the individual chains decreases, and the effect of the fixed substrate on the gel properties should also increase. Specifically, the length scale of the constraint is likely to be influenced by the degree of cross-linking, and because only the gel−substrate interface is probed by these measurements, the substrate effect on this region could vary with cross-linking density. This may explain why the transition temperatures for 3.5 and 8.6 mM BIS are similar to the bulk gel values while the sample with 15 mM BIS has an elevated transition temperature. Conversely, the effect of the increased SA concentration is to increase the osmotic pressure of the counterions, and this causes swelling in bulk gels. The gel also becomes more hydrophilic, causing the transition temperature to increase. This should have a similar effect on bulk gels and thin films, although the magnitude of the change in the transition temperature varies somewhat, as shown by the data in Table 1.

Film Thickness. From macroscopic observations[25] it is known that NIPAAm gel films on the order of 50 μm thick show significant distortion as they expand and contract in response to temperature, and these transitions cannot be viewed as one-dimensional. Most likely, there is a characteristic length scale over which the effects of the substrate are felt by the gel film. To explore this further, a separate set of experiments used a surface-bound photoinitiator so that the thickness of the gel layer could be controlled by the UV exposure time.[38] This was used to produce 0.3 μm and thinner films, which is on the order of the decay length of the SPR measurement, and thus the entire film is probed by this set of measurements. The transition temperatures of the thin gel films correspond well to those at the NIPAAm−substrate interface (see Table 1), and the constraint of the fixed substrate then appears to affect the entire film. This does not resolve the issue of the exact length scale needed to describe the system, but we can conclude that the constraint of the substrate is felt by the film over distances larger than the decay length of the surface plasmon. A more detailed study of gel film swelling behavior as a function of film thickness will be published separately.[17,43]

Pressure Effects. The data in Figure 3 show the transition temperatures of the samples in Table 1 (4 μm) as a function of pressure. From these data, it is clear that the pressure sensitivity of the volume phase transition temperature at the NIPAAm−substrate interface is similar to that of bulk gels.[13,14] The transition temperatures at 1 bar differ from those of bulk gels of the same composition, as shown in Table 1. However, the additional increase in the transition temperature due to hydrostatic pressure corresponds well to the behavior of bulk gel. It is tempting to try and model the constraint as an added stress or pressure within the gel,[44] but this is inconsistent with the data in these experiments. In terms of the sigmoidal fit, the constraint has been shown to affect the transition temperature T but not the width of the transition ΔT, while added hydrostatic pressure is shown to affect both T and ΔT.

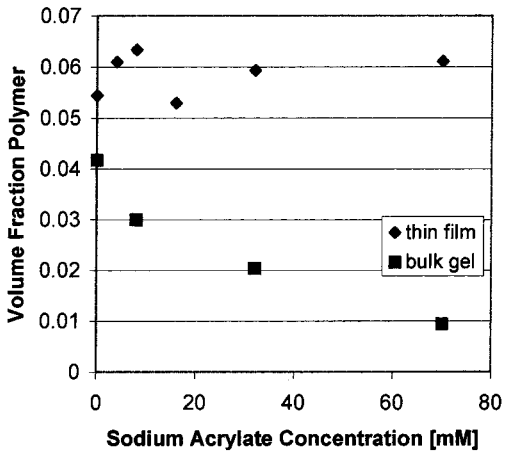

Figure 4. Equilibrium swelling of 4 μm films and bulk gel at temperatures below the volume phase transition temperature as a function of the ionizable comonomer concentration. The volume fraction of polymer in the gel samples is calculated from the refractive index in the case of the thin film and from the equilibrium swelling ratio in the case of the bulk gel.

Equilibrium Swelling. The polymer volume fraction of the gel films can be calculated from the refractive index of the film. In bulk gel, the addition of an ionizable comonomer swells the gel significantly and the polymer volume fraction decreases. At temperatures below the volume phase transition temperature, this results in a dramatic increase in the equilibrium swelling ratio with increased ionic content.[9] However, it is apparent from the data in Figure 4 that the swelling ability of counterions in the thin film is substantially less than in the bulk, and the polymer volume fraction does not appear to change as a function of sodium acrylate concentration. The total volume change can be estimated from the change in the equilibrium swelling ratio in the case of bulk gels and from the change in refractive index in the case of gel films. While the volume phase transition of the corresponding bulk gels can have a total volume change as large as 100-fold, the gel films have a total volume change around 15-fold. Thus, ionized gels in this confined geometry have increased transition temperatures with increased ionic content, as in the case of bulk gels, but the associated swelling of the gel at temperatures below the transition temperature is not present.

Similar results have been found for thermoresponsive core−shell colloids with a solid latex core and a cross-linked NIPAAm shell.[32,33] The presence of a fixed substrate limits the degree of swelling at low temperatures but also prevents the shell from fully collapsing at high temperatures. The limited swelling at low temperatures is illustrated in Figure 4, but the refractive index at high temperatures (Figure 1B) is in good agreement with a fully collapsed gel film. As a result, there does not appear to be any effect on the degree of swelling at high temperatures for the range of film thicknesses observed here. As a thought experiment, a one-dimensional analogue to Flory−Tanaka theory should have a more rapid increase in elasticity free energy as the gel expands and polymer volume fraction decreases. This could explain the reduced swelling for the gel at the NIPAAm−substrate interface, but it is unclear how this will affect the volume phase transition temperature and the width of the transition. Current theory has successfully described the volume phase transition in both two and three dimensions, but it is unable to capture all the characteristics of this system.

Conclusions

This is a first step in understanding the volume phase transition in NIPAAm gels under lateral constraint. This is particularly relevant for a number of applications such as thermally selective membrane separations[7] and thermally activated surfaces in biomaterials.[8] These applications use thermoresponsive hydrogels at surfaces and at interfaces, and the understanding of bulk hydrogels cannot necessarily be extended to these types of geometries.

As demonstrated in this paper, NIPAAm gel at a fixed interface is a complex system, and the confinement of the gel is likely limited to some characteristic length scale or distance from the interface. The data also suggest that the constraint cannot simply be modeled as an added stress or pressure within the material. However, we have shown that the effect of confinement on NIPAAm at a fixed interface is to alter the transition temperature, especially for ionized or highly cross-linked gels, and to significantly decrease the swelling ability of ionic species in the gel. Furthermore, the effect of increased hydrostatic pressure is to increase the transition temperature and the width of the transition, similar to bulk gels. This causes interesting phase behavior in that under certain conditions the gel can expand in response to increased pressure.

Acknowledgment. This work was supported by a Max-Planck-Research School for Polymer Materials Science fellowship (T.J.), an NSF Graduate Research Fellowship (M.E.H.), and the Center on Polymer Interfaces and Macromolecular Assemblies (CPIMA), which is sponsored by the NSF-MRSEC program under DMR 9808677.

References and Notes

(1) Eichenbaum, G. M.; Kiser, P. F.; Simon, S. A.; Needhan, D. *Macromolecules* **1998**, *31*, 5084−5093.
(2) Hirokawa, Y.; Tanaka, T. *J. Chem. Phys.* **1984**, *81*, 6379−6380.
(3) Kato, N.; Yamanobe, S.; Takahashi, F. *Mater. Sci. Eng., C* **1997**, *5*, 141−147.
(4) Shiga, T. *Adv. Polym. Sci.* **1997**, *134*, 131−163.
(5) Dong, L. C.; Hoffman, A. S. *J. Controlled Release* **1990**, *31*, 21−31.
(6) Kato, N.; Yamanobe, S.; Takahashi, F. *Mater. Sci. Eng., C* **1997**, *5*, 141−147.
(7) Reber, N.; Spohr, R.; Wolf, A.; Omichi, H.; Tamada, M.; Yoshida, M. *J. Membr. Sci.* **1998**, *140*, 275−281.
(8) Okano, T.; Yamada, N.; Okuhara, M.; Sakai, H.; Sakurai, Y. *Biomaterials* **1995**, *16*, 297−303.
(9) Shibayama, M.; Tanaka, T. *Adv. Polym. Sci.* **1993**, *109*, 1−62.
(10) Suzuki, A.; Kojima, S. *J. Chem. Phys.* **1994**, *101*, 10003−10007.
(11) Suzuki, A.; Sanda, K.; Omori, Y. *J. Chem. Phys.* **1997**, *107*, 5179−5185.
(12) Plate, N. A.; Lebedeva, T. L.; Valuev, L. I. *Polym. J.* **1999**, *31*, 21−27.
(13) Kato, E. *J. Chem. Phys.* **1997**, *106*, 3792−3797.
(14) Nakamoto, C.; Kitada, T.; Kato, E. *Polym. Gels Networks* **1996**, *4*, 17−31.
(15) Kato, E.; Kitada, T.; Nakamoto, C. *Macromolecules* **1993**, *26*, 1758−1760.
(16) Grinberg, N. V.; Dubovik, A. S.; Grinberg, V. Y.; Kuznetsov, D. V.; Makhaeva, E. E.; Grosberg, A. Y.; Tanaka, T. *Macromolecules* **1999**, *32*, 1471−1475.
(17) Kuckling, D.; Harmon, M. E.; Frank, C. W. *Macromolecules*, in press.
(18) Yamazaki, Y.; Tada, T.; Kunugi, S. *Colloid Polym. Sci.* **2000**, *278*, 80−83.
(19) Gehrke, S. H.; Palasis, M.; Akhtar, M. K. *Polym. Int.* **1992**, *29*, 29−36.
(20) Tanaka, T. *Phys. Rev. Lett.* **1978**, *40*, 820−823.
(21) Knoll, W. *Annu. Rev. Phys. Chem.* **1998**, *49*, 569−638.
(22) Prucker, O.; Christian, S.; Beck, H.; Ruhe, J.; Frank, C. W.; Knoll, W. *Macromol. Chem. Phys.* **1998**, *199*, 1435−1444.
(23) Wischerhoff, E.; Zacher, T.; Laschewsky, A.; Rekai, E. D. *Angew. Chem., Int. Ed.* **2000**, *39*, 4602−4604.
(24) Peng, B.; Johannsmann, D.; Rühe, J. *Macromolecules* **1999**, *32*, 6759−6766.
(25) Hoffman, J.; Plotner, M.; Kuckling, D.; Fischer, W.-J. *Sens. Actuators, A* **1999**, *77*, 139−144.
(26) Pan, Y. V.; Wesley, R. A.; Luginbuhl, R.; Denton, D. D.; Ratner, B. D. *Biomacromolecules* **2001**, *2*, 32−36.
(27) Yakushiji, T.; Sakai, K. *Langmuir* **1998**, *14*, 4657−4662.
(28) Okano, T.; Kikushi, A.; Sakurai, Y.; Takei, Y.; Ogata, N. *J. Controlled Release* **1995**, *36*, 125−133.
(29) Liang, L.; Feng, X.; Liu, J.; Rieke, P. C. *J. Appl. Polym. Sci.* **1999**, *72*, 1−11.
(30) Liang, L.; Feng, X.; Liu, J.; Rieke, P. C.; Fryxell, G. E. *Macromolecules* **1998**, *31*, 7845−7850.
(31) Zhu, P. W.; Napper, D. H. *Macromol. Chem. Phys.* **1999**, *200*, 698−705.
(32) Kim, J.; Deike, I.; Dingenouts, N.; Norhausen, C.; Ballauff, M. *Macromol. Symp.* **1999**, *142*, 217−225.
(33) Seelenmeyer, S.; Deike, I.; Rosenfeldt, S.; Norhausen, C.; Dingenouts, N.; Ballauff, M.; Narayanan, T.; Lindner, P. *J. Chem. Phys.* **2001**, *114*, 10471−10478.
(34) Revzin, A.; Russell, R. J.; Yadavalli, V. K.; Koh, W. G.; Deister, C.; Hile, D. D.; Mellott, M. B.; Pishko, M. V. *Langmuir* **2001**, *17*, 5440−5447.
(35) Amarego, W. L. F.; Perrin, D. D. *Purification of Laboratory Chemicals*; Butterworth-Heineman: Boston, MA, 1996.
(36) Kambhampati, D. K.; Jakob, T. A. M.; Robertson, J. W.; Cai, M.; Pemberton, J. E.; Knoll, W. *Langmuir* **2001**, *17*, 1169−1175.
(37) Zheng, J. J.; Odake, T.; Kitamori, T.; Sawada, T. *Anal. Chem.* **1999**, *71*, 5003−5008.
(38) Prucker, O.; Schimmel, M.; Tovar, G.; Knoll, W.; Rühe, J. *Adv. Mater.* **1998**, *10*, 1073−1077.
(39) Kleideiter, G.; Lechner, M. D.; Knoll, W. *Macromol. Chem. Phys.* **1999**, *200*, 1028−1033.
(40) Hirotsu, S.; Yamamoto, I.; Matsuo, A.; Okajima, T.; Furukawa, H.; Yamamoto, T. *J. Phys. Soc. Jpn.* **1995**, *64*, 2898−2907.
(41) Schmidt, M.; Maurer, F. H. J. *J. Polym. Sci., Part B* **1998**, *36*, 1061−1080.
(42) Eisenberg, H. *J. Chem. Phys.* **1965**, *43*, 3887−3892.
(43) Harmon, M. E.; Kuckling, D.; Frank, C. W. Manuscript in preparation.
(44) Zhao, J.-H.; Kiene, M.; Hu, C.; Ho, P. S. *Appl. Phys. Lett.* **2000**, *77*, 2843−2845.

MA010985K